

# Effects of processing parameters on fatigue properties of LY2 Al alloy subjected to laser shock processing

Lei Zhang (张磊), Jinzhong Lu (鲁金忠)\*, Yongkang Zhang (张永康), Kaiyu Luo (罗开玉), Fengze Dai (戴峰泽), Chengyun Cui (崔承云), Xiaoming Qian (钱晓明), and Junwei Zhong (钟俊伟)

School of Mechanical Engineering, Jiangsu University, Zhenjiang 212013, China

\*Corresponding author: bluesky2005@163.com

Received December 22, 2010; accepted January 20, 2011; posted online May 12, 2011

We address the effects of processing parameters on residual stresses and fatigue properties of LY2 Al alloy by laser shock processing (LSP). Results show that compressive residual stresses are generated near the surface of samples due to LSP. The maximum compressive residual stress at the surface by two LSP impacts on one side is higher than that by one LSP impact. The maximum value of tensile residual stress is found at the mid-plane of samples subjected to two-sided LSP. Compared with fatigue lives of samples treated by single-sided LSP, lives of those treated by two-sided LSP are lower. However, these are higher than untreated ones.

OCIS codes: 140.3390, 240.6690, 350.3850.

doi: 10.3788/COL201109.061406.

LY2 Al alloy is a heat-resistant hard Al with moderate strength and light weight, widely used in the aerospace and automotive industries<sup>[1]</sup>. By analysis of the failure blades, fracture occurs because the cracks generated on the surface can reduce the fatigue strength<sup>[2]</sup>. To avoid the early failure of the blades, shot peening has been used in improving the surface integrity to enhance the fatigue strength. High-intensity shot peening and low-plasticity burnishing have been used to treat the edges of blades, which can improve the fatigue-resistance strength and the fatigue lives<sup>[2,3]</sup>. Laser shock processing (LSP) is a new and promising surface treatment technique to improve the fatigue durability, wear resistance, and other mechanical properties of metals and alloys. During the process, the generated shock wave can introduce deep compressive residual stresses into the materials<sup>[4–7]</sup>.

Considerable research has been carried out to examine the effects of LSP on mechanical properties and fatigue lives of Al alloys<sup>[8–14]</sup>. For example, the effects of a single LSP on residual stress distribution in 7085-T7651 Al alloy have been exhibited<sup>[8]</sup>. Moreover, the high-level compressive residual stresses produced in Al alloys during LSP as well as the improvement in fatigue life made by the compressive stress magnitude have been investigated<sup>[10]</sup>. The relationship between the principal residual stresses and the depth of the 6061-T6 Al sample by LSP has been established<sup>[13]</sup>. Moreover, the geometrical effects on residual stresses in 7050-T7451 Al alloy rods subjected to LSP have been explored<sup>[14]</sup>. Most of the above studies showed that the mechanical properties and fatigue lives improved significantly for Al alloys because of the compressive residual stresses after LSP. However, few studies have focused on the effects of two-sided LSP on the distribution of the residual stresses, especially along the direction of the depth.

In this letter, we investigate the residual stress field and fatigue property of LY2 Al alloy by single-sided and two-sided LSPs. We study the effect of the processing parameter, such as the LSP impact time used in LSP on the residual stress, and evaluated the low cyclic fatigue (LCF) property on the samples manufactured by LY2 Al

alloy. Lastly, we examine and discuss the mechanism of the LSP effect with different processing parameters on the residual stress field and fatigue property.

LY2 Al alloy was cut into tensile samples with a dog-bone shape from the same metal plane, as shown in Fig. 1. The chemical compositions and mechanical properties of LY2 Al alloy are shown in Tables 1 and 2, respectively.

The single-sided LSP process and the schematic diagrams were detailed clearly in literature<sup>[1,15,16]</sup>. In LSP, the shock waves were induced by a Q-switched repetition-rate laser with a wavelength of 1,054 nm, pulse of approximately 20 ns, spot diameter of 5 mm, and repetition rate of 0.5 Hz. The water with a thickness of 1–2 mm was used as the transparent overlay, and the 7075 Al foil with a thickness of 50  $\mu\text{m}$  was used as the opaque overlay to protect the blade surface from thermal effect. Laser energy was approximately 25 J, and the power density at the LY2 Al alloy surface was approximately 5 GW/cm<sup>2</sup>.

The high-energy laser pulse is split into two and simultaneously focused on two sides of the thin sections of the samples. The other procedures, such as use of transparent overlay and opaque overlay are the same as in the process of LSP. Experiments on this subject were conducted by Clauer *et al.* in 2001<sup>[17]</sup>.

According to the different processing parameters of LSP, the treated samples were divided into three groups. For the first group, only one side of the sample was subjected to single laser impact. For the second group, one side of the sample was treated with two laser impacts. These two groups belonged to single-sided LSP. For the third group, two sides of the sample underwent single laser impact simultaneously. The group belonged to two-sided LSP.

The residual stress, through the direction of the depth, was determined by using X-ray diffraction (XRD) with  $\sin^2\psi$  method. X-ray beam diameter was approximately 2 mm, its source was CrK $\alpha$  ray, and the diffraction plane was  $\alpha$  phase (420) plane. The Poisson's ratio was set as 0.30 in the stress calculation. The feed angle of the ladder scanning was 0.1°/s, and the scanning start angle and

**Table 1. Chemical Composition of LY2 Al Alloy**

Composition	Cu	Mg	Mn	Be	Si	Fe	Cr	Zn	Ti	Al
Percent (wt.-%)	2.6–3.22	2.0–2.4	0.45–0.7	0.05	0.3	0.3	0.05	0.05	0.15	other

**Table 2. Mechanical Properties of LY2 Al Alloy**

Type	Value
Specific Gravity $d$ (g/cm <sup>3</sup> )	2.8
Tensile Strength $\delta b$ (kgf/mm <sup>2</sup> )	470
Elongation $\delta$ (%)	14
Vickers Hardness (HV)	120

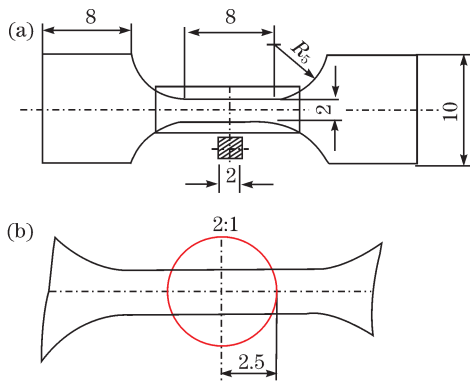


Fig. 1. Dimensions of the measured sample subjected to LSP (unit: mm). (a) Tensile sample; (b) partial enlarged drawing of the treated area subjected to LSP.

termination angle were 159° and 168°, respectively. Thin layers of the sample surface were successively removed by electrolytic polishing to obtain the depth profile of the residual stress.

Before fatigue tests, several samples were treated by single-sided and two-sided LSPs. The regions subjected to LSP are schematically shown in Fig. 1(b). A total of four groups of the samples were used in the fatigue tests to investigate the effect of the processing parameter on the fatigue performance of the samples during LSP. The above-mentioned three groups were included, and the fatigue property of the untreated samples as the fourth group was also evaluated for comparison.

The axial LCF tests were performed on a MTS880-10 servo-hydraulic material testing machine system at room temperature. During LCF tests, the load ratio was maintained at  $R = 0.2$  and the frequency of 1.5 Hz with a sine waveform was used. The maximum applied stress  $\sigma_{max}$  was kept at 255 MPa.

The residual stresses along the depth direction after single-sided LSP and two-sided LSP treatments are shown in Fig. 2. The value of the residual stress without any treatment can be considered as zero. Firstly, the compressive residual stresses exist in the subsurface and the maximum values are located at the surface. After one LSP impact, the maximum compressive residual stress is -150 MPa. Subjected to two LSP impacts on one side, the maximum compressive residual stress is approximately -220 MPa. However, after two-sided LSP impacts, the maximum compressive residual stress is

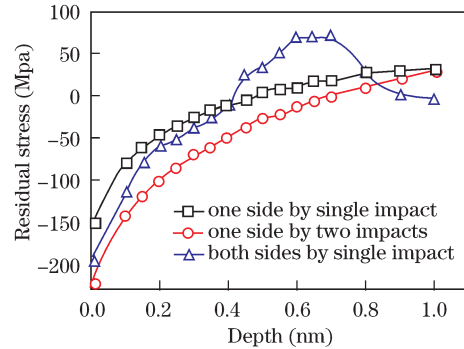


Fig. 2. Residual stresses of different technological parameters along the depth direction.

-195 MPa. The maximum value of compressive residual stress of the second group increased by 46.67% compared with the first group. The maximum value of compressive residual stress of the third group is lower than that of the second group but higher than that of the first group. Hence, with the increase in the number of LSP impact, the maximum value of compressive residual stresses increases. However, the effects obtained by two-sided LSP are not superior to that of two LSP impacts on one side.

Secondly, as shown in Fig. 2, the tensile residual stresses are generated at the mid-plane of the samples. After one LSP impact, the maximum value of tensile residual stress is 30 MPa at a depth of 1.0 mm. After two LSP impacts on one side, the maximum value of tensile residual stress is approximately 29.9 MPa at the depth of 1.0 mm from the top surface. However, after two-sided LSP impacts, the maximum value of tensile residual stress is 70 MPa at the depth of 0.70 mm from the top surface. Consequently, the tensile residual stress is changed into the compressive stress of -1 MPa at the middle of the depth, 1.0 mm, from the top surface. However, the compressive residual stress is considerably lower than the tensile residual stress. The values of the tensile residual stresses gained by single-sided LSP are almost the same, but lower than those of two-sided LSP. Between the surface and the mid-plane, the curve of the third group in Fig. 2 is a slightly steeper among the three groups. The thinner the samples, the more obvious the phenomenon becomes. Ding *et al.* have performed finite element method (FEM) simulation analyses on the residual stresses along three different thicknesses of thin sections of Ti-6Al-4V alloy as a result of two-sided LSP impacts<sup>[18]</sup>.

The fatigue lives of the treated samples using LSP with different processing parameters as well as the untreated sample are shown in Fig. 3. The samples treated with two LSP impacts on one side clearly exhibit the highest fatigue life. By comparing with the untreated sample, the fatigue lives of the samples increased by 116.7% and 125% after the single LSP impact and two LSP impacts on one side, respectively. Moreover, the fatigue life of the samples after two LSP impacts is longer compared

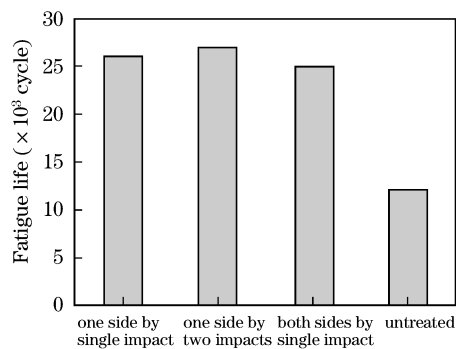


Fig. 3. Fatigue property comparison with different LSP parameters.

with the after one laser LSP impact on one side.

This phenomenon is attributed to two reasons. On one hand, because of the surface irradiated by the laser, the subsurface material is submitted to an elastoplastic wave, which generates uniaxial plastic strain. The surrounding material is opposed to the strain and induces biaxial compressive residual stresses after the interaction<sup>[19]</sup>. The compressive residual stresses with values of several hundred megapascals are generated near the specimen surface after LSP. In addition, the compressive surface layer restrains the initiation and growth of the fatigue cracks mostly originating from the material surface<sup>[12]</sup>. On the other hand, the magnitude of the compressive stresses is higher for two impacts than for one impact. Hence, LSP with both processing parameters can improve the capability to restrain the fatigue cracks. However, the depth of the compressive stresses is normally unchanged in the LSP impacts under both processing parameters<sup>[20,21]</sup>.

Figure 3 shows that the fatigue life of the sample after two-sided LSP impact is higher than that of the untreated sample, but lower than that after single-sided LSP impact. After two-sided LSP impact, the layers with compressive residual stress are generated at both sides of the sample, which can also inhibit most fatigue cracks from occurring at material surface. Nevertheless, the tensile residual stresses will be enhanced significantly at the mid-thickness of the samples due to the overlapping of the two same shock waves from the reserve direction. Consequently, the potential cracks in the inner materials are generated, which decreases the material fatigue lives to a certain degree.

The mechanism of the fatigue property by the single-sided LSP impact is explained by residual stress generation. The material surface is irradiated by laser shock wave. The residual stress of the impacted surface is a tensile stress state due to the propagation of laser shock wave, which results in material plastic deformation<sup>[22,23]</sup>. As the shock waves propagate into the material, plastic deformation occurs to a depth at which the peak pressure no longer exceeds the Hugoniot elastic limit of the material. Residual stresses are induced throughout the affected depth<sup>[24]</sup>. The corresponding experimental data are shown in Fig. 2; the affected depth of the compressive residual stresses of the first group and the second group are approximately 0.5 and 0.7 mm, respectively; and the leaving depth belongs to the affected depth of the tensile residual stress. Then, laser ablation stops. Due to the material reaction at the impact plane, the

surrounding material is opposed to the strain brought about by the change of volume and reverts to the former size. When the dynamic stresses of shock waves within a material are above its dynamic yield strength, plastic deformations occurs. This continues until the peak dynamic falls below the dynamic yield strength. The plastic deformation induced by the shock waves results in strain hardening and compressive residual stresses at the material surface<sup>[25–27]</sup>. Biaxial compressive residual stresses are induced<sup>[22,23]</sup>.

Residual stresses after LSP are the stresses remaining in a metal after the shock waves are dispersed. These residual stresses play an important role in enhancing the fatigue properties of metallic materials<sup>[28]</sup>.

With the increase in depth, the value of compressive residual stresses decreases until zero. Subsequently, the compressive residual stresses are transformed into tensile residual stresses to balance the mechanical system in the inner material and keep the whole material stable<sup>[1,7,29]</sup>.

Our experimental result is similar to the result of this model. In Fig. 2, the residual stress value of the first group and the second group is negative at the depth of 0.5 and 0.7 mm. Value becomes positive to balance the high compressive stress value up to a low depth.

During two-sided LSP, surface and bottom of the thin sample with the thickness of 2 mm are shocked by the two laser beams simultaneously, thus there are two shock waves propagating from opposite directions simultaneously. However, after a propagating period, both may encounter each other and some parts of the waves will cancel each other out because of the simultaneous work of the two opposite shock waves. This causes the value of surface compressive residual stress to decrease and the value of tensile residual stresses at the mid-plane to increase sharply. This phenomenon almost occurred in the experiment. As seen in Fig. 2, the value of the compressive residual stress layer of the third group is lower than that of the second group, although the total number of LSP impacts is two. In addition, the affected depth of the compressive residual stress layer of the third group is the shallowest among the three groups. The tensile residual stress value of the third group within the material is the largest among the groups and increases sharply compared with the value of the compressive residual stress itself near the surface. Thus, the capability to restrain the surface crack initiation and propagation is reduced, while the increasing tensile residual stresses in the mid-plane cause inner crack propagation. As a result, the fatigue property of the sample by two-sided LSP impact is lower than that by single-sided LSP impact (Fig. 3).

The reason for the decrease in fatigue life of the sample by two-sided LSP is explained by the simplified model shown in Fig. 4. The tensile residual stress in the mid-plane was found to increase because of the counterbalance of the shock waves from the opposite directions. The experimental data are shown in Fig. 2. The affected range of the tensile residual stress of the third group is wide, with the depth of 0.4–0.9 mm approximately, while the tensile residual stress value of the third group is large comparatively. In addition, the samples with the thickness of 2 mm belong to the thin sheet and a certain disadvantageous counterbalance of the tensile residual stress between the frontal and reversed shocks exists.

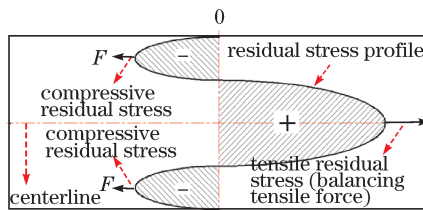


Fig. 4. Model of residual stresses induced by two-sided LSP along the direction of the depth.

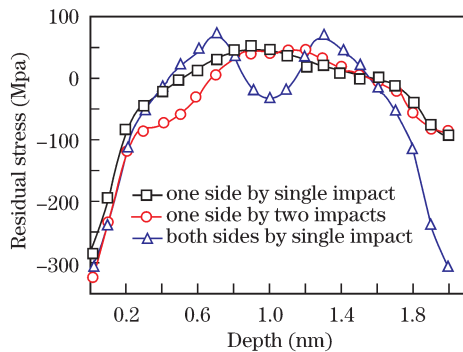


Fig. 5. Simulation of the residual stresses along the depth direction under different technological parameters.

Figure 5 shows the simulated residual stresses along the depth direction under different processing parameters by ABAQUS. With the increment of the LSP impact time, the maximum value of the compressive stress increases. The tensile residual stresses appear almost at the mid-plane of the samples. The value of tensile residual stress of the third group is the highest among the three groups. The compressive stresses of the third group occur in the mid-plane. Similar result is obtained by the experimental data shown in Fig. 2.

In conclusion, LSP is considered as one of the most promising techniques because of its ability to induce the deeper compressive residual stresses and to enhance the fatigue property of the metal component. The effect of LSP with different processing parameters on the residual stresses and fatigue property is investigated. Compressive residual stress layer is generated at the surface layer of LY2 Al alloy. The fatigue life of the samples by two LSP impacts at one side is higher than that by one laser impact. The fatigue lives of the samples by two-sided LSP are lower than those by single-sided LSP, but higher than those of the untreated samples. The inner tensile residual stresses at the mid-plane of the treated samples increase and their fatigue lives decrease.

This work was supported by the National Natural Science Foundation of China under Grant Nos. 50705038 and 50735001.

## References

- J. Z. Lu, K. Y. Luo, Y. K. Zhang, C. Y. Cui, G. F. Sun, J. Z. Zhou, L. Zhang, J. You, K. M. Chen, and J. W. Zhong, *Acta Mater.* **58**, 3984 (2010).

- M. P. Pawar and G. Ranjan, *Compos. Sci. Technol.* **65**, 581 (2005).
- A. King, A. Steuwer, C. Woodward, and P. J. Withers, *Mater. Sci. Eng. A* **435-436**, 12 (2006).
- M. A. Meyers, F. Gregori, B. K. Kad, M. S. Schneider, D. H. Kalantar, B. A. Remington, G. Ravichandran, T. Boehly, and J. S. Wark, *Acta Mater.* **51**, 1211 (2003).
- W. Li, W. He, Y. Li, C. Wang, and Z. Yang, *Chinese J. Lasers* (in Chinese) **36**, 2197 (2009).
- B. S. Yilbas, S. Z. Shuja, A. Arif, and M. A. Gondal, *J. Mater. Process. Technol.* **135**, 6 (2003).
- C. S. Montross, W. Tao, Y. Lin, G. Clark, and Y.-W. Mai, *Int. J. Fatigue* **24**, 1021 (2002).
- H. Luong and M. R. Hill, *Mater. Sci. Eng. A* **477**, 208 (2008).
- Y. K. Zhang, X. R. Zhang, X. D. Wang, S. Y. Zhang, C. Y. Gao, J. Z. Zhou, J. C. Yang, and L. Cai, *Mater. Sci. Eng. A* **297**, 138 (2001).
- C. Rubio-González, J. L. Ocaña, G. Gomez-Rosas, C. Molpeceres, M. Paredes, A. Banderas, J. Porro, and M. Morales, *Mater. Sci. Eng. A* **386**, 291 (2004).
- X. Luo, J. Zhang, G. Zhao, X. Ren, and Y. Zhang, *Chin. J. Lasers* (in Chinese) **36**, 3323 (2009).
- P. Peyre, R. Fabbro, P. Merrien, and H. P. Lieurade, *Mater. Sci. Eng. A* **210**, 102 (1996).
- G. Gomez-Rosas, C. Rubio-Gonzalez, J. L. Ocaña, C. Molpeceres, J. A. Porro, W. Chi-Moreno, and M. Morales, *Appl. Surf. Sci.* **252**, 883 (2005).
- C. Yang, P. D. Hodgson, Q. Liu, and L. Ye, *J. Mater. Process. Technol.* **201**, 303 (2008).
- J. Lu, "Investigation of laser shock processing on the mechanical properties and micro-plastic deformation mechanism of LY2 aluminum alloy" (in Chinese), PhD. Thesis (Jiangsu University, 2010).
- T. S. Srivatsan, *Mater. Des.* **23**, 141 (2002).
- A. H. Clauer and D. F. Lahrman, *Key Eng. Mater.* **197**, 121 (2001).
- K. Ding and L. Ye, *Surf. Eng.* **19**, 127 (2003).
- M. Ni, J. Zhou, C. Yang, X. Zhang, and J. Du, *Laser J.* (in Chinese) **27**, 79 (2006).
- M. Ni, J. Zhou, C. Yang, H. Liu, J. Du, and X. Zhang, *Appl. Laser* (in Chinese) **26**, 73 (2006).
- Y. K. Zhang, J. Z. Lu, X. D. Ren, H. B. Yao, and H. X. Yao, *Mater. Des.* **30**, 1697 (2009).
- S. Huang, J. Zhou, S. Jiang, Y. Zhu, and L. Hu, *Chinese J. Lasers* (in Chinese) **37**, 256 (2010).
- Y. Hu, C. Gong, Z. Yao, and J. Hu, *Surf. Coat. Technol.* **203**, 3503 (2009).
- P. Peyre, L. Berthe, X. Scherpereel, and R. Fabbro, *J. Mat. Sci.* **33**, 1421 (1998).
- A. F. M. Arif, *J. Mater. Process. Technol.* **136**, 120 (2003).
- P. Peyre and R. Fabbro, *Opt. Quant. Electron.* **27**, 1213 (1995).
- J. L. Ocaña, M. Morales, and C. Molpeceres, J. Torres, *Appl. Surf. Sci.* **238**, 242 (2004).
- B. Han and D. Y. Ju, *Mater. Des.* **30**, 3325 (2009).
- Q. Xiao, S. Shao, J. Shao, and Z. Fan, *Chin. Opt. Lett.* **7**, 162 (2009).